A New Method for Simultaneously Determining The Magnitude And Orientation of SH_{max} And Rock Strength Using Wellbore Failures in Deviated Wells[1]

Lei Jin

Department of Geophysics, Stanford University, California

leijin@alumni.stanford.edu

ABSTRACT

Forward constraining of the magnitude of S_{Hmax} on a stress polygon using wellbore failures observed from deviated wells requires the orientation of S_{Hmax} known *a priori*. This orientation can be separately determined from, e.g., wellbore failures in vertical/near-vertical wells. Unfortunately, in the case where image logs are available only in highly deviated wells, S_{Hmax} orientation cannot be independently determined as the impact of wellbore trajectory on wellbore failures can be significant. In this study, we propose a new method for simultaneously determining the magnitude and orientation of S_{Hmax} as well as two rock strength variables using wellbore failures in arbitrarily deviated wells. This method fully accounts for the inter-dependence among the unknown variables and fully considers the impact of wellbore trajectory on wellbore failures. It is associated with two key assumptions: (1) the size of the breakout coincides with the plastic yield zone; (2) the stress redistribution due to plastic strain is negligible, and the yield function reaches a maximum value at the breakout center and reaches zero at the breakout edges. Based on these assumptions, we set up a constrained optimization at each breakout. The objective function is chosen based on the yield function at the breakout center, and the constraints are imposed based on frictional equilibrium, the presence or lack of drilling induced tensile fractures, and the breakout width. The Drucker-Prager yield criterion and the 3D Griffith tensile failure criterion were chosen for our method. We then employ the interior-point algorithm for performing the optimization and compute the Hessian matrix using the quasi-Newton method for second-derivative test and selection of the local extremum. This optimization process can be easily executed for all breakouts. Finally, we demonstrate the application of our new method using breakout data from a deviated wellbore and show that it is able to overcome the limitations of the conventional method

Key words: in Geophysics -situ stress, SH_{max}, frictional strength, constrained optimization

---

1. INTRODUCTION

Knowledge of the magnitude and orientation of S_{Hmax} is critical to geomechanical studies. These two variables are usually determined from analyzing drilling-induced wellbore failures, including breakout and tensile fractures. In vertical wells, the complexity of the problem greatly reduces as all the shear stresses on the wellbore wall vanish (if assuming the in-situ principal stresses are always along the vertical and horizontal directions). As a result, drilling-induced wellbore failures are directly indicative of the orientation of S_{Hmax}, and its magnitude can be predicted from breakout size using closed-from analytical solutions that are based on a selected failure criterion, e.g., the uniaxial compressive failure criterion (Barton et. al., 1998), or the Mohr-Coulomb shear failure criterion (Vecchia et. al., 2014). The problem becomes much more complex when analyzing drilling-induced wellbore failures in deviated wells. Given independent knowledge of overburden, S_{hmin} and pore pressure, and assuming that the state of stress is limited by frictional strength of earth crust at depth (Towend and Zoback), the magnitude of S_{Hmax} can be constrained within a range of uncertainty. The width of this range can be further narrowed based on: (1) the presence or lack of drilling-induced tensile fractures (DITF), by employing certain tensile failure criteria; and (2) breakout widths, assuming that the stress concentration at the edge of a breakout is in equilibrium with the rock strength (Zoback, 2010). Despite the prevalence of this approach, it is subjected to a few limitations. First, the orientation of S_{Hmax} is required to be known *a priori* (Peska and Zoback, 1995). But this generally cannot be independently determined, as the impact of wellbore trajectory on wellbore failures can be significant and must be taken into account (Mastin, 1988). Thus a good matching with the observation of drilling-induced wellbore failures can only be accomplished through a forward trail-and-error process. Second, knowledge of rock strength is required for selecting the appropriate contour lines. Third, the forward approach needs to be repeated manually for each wellbore failure; this makes it impractical when dealing with large quantities of wellbore failure data.

Alternative approaches, based on information provided by drilling-induced wellbore failures or hydraulic fractures, have been proposed to determine the full in-situ stress tensor or some of its components. For example, using breakouts from multiple wells that are in close proximity but with different deviations, Zajac and Stock (1997) developed an inversion technique for determining the directions of the three principal stresses and their relative magnitudes. Unfortunately, measurements with such a configuration are mostly unavailable. Djurhuus and Aadnoy (2003) proposed a direct linear inversion method for determining the magnitudes of S_{Hmax} and Sh_{min} using solely tensile fractures. A set of linearized fracturing equations is established by neglecting wellbore shear stresses, thus the method is appropriate when wellbore is along one of the principal in-situ stresses. Thorsen (2011) assumes that the selected tensile failure function is maximal along the tensile fracture traces, allowing determination of the magnitudes of S_{hmin} and S_{Hmax} through maximization of a generalized

failure function. Based on a different objective function, Synn et. al (2015) utilized an nonlinear optimization routine to recover the full stress tensor using hydraulic fracture data collected from multiple inclined boreholes.

In this study, we propose a new method for simultaneously determining the magnitude and orientation of S_{Hmax} as well as two rock strength variables, UCS and internal frictional angle, from breakout data observed from an arbitrarily deviated well. This method is designed for the case where images logs are not available from multiple deviated wells with different deviations, and where breakouts are more prominent than tensile fractures, and that independent knowledge of S_{hmin}, pore pressure and overburden is available. The method fully considers the inter-dependence of the unknown variables and the impact of wellbore trajectory on wellbore failures. The process is easily repeatable and is advantageous in dealing large quantities of breakout data.

2. ELASTIC STRESS STATE AROUND A DEVIATED CYLINDRICAL WELLBORE

Four coordinates systems are used for this study (see figure 1). The first is a in-situ principal stress Cartesian coordinate system x-y-z in which x is along one of the S_{hmin} directions, y is along one of the S_{Hmax} directions and z is pointing upward. The second is a local wellbore Cartesian coordinates system x'-y'-z' in which x' is pointing from the center of the wellbore cross-section towards the wellbore bottom, y' is along the intersecting line of the cross-section and the horizontal plane at that depth, and z' is along the wellbore axis. For uniqueness, both x-y-z and x'-y'-z' obey right-hand rule. The third is a local wellbore cylindrical coordinate system r-θ-z' in which r is the radial direction, θ is the angle with respect to x' in an anticlockwise sense, and z' is along the wellbore axis. Note that x-y-z is depth-dependent due to the stress heterogeneity, and x-y'-z' and r-θ-z' depends on the wellbore trajectory. The fourth is the geographic coordinate system. Also, in figure 1, δ is the dipping angle of the wellbore, and ϕ represents the angle formed by y' and y projected on a horizontal plane, and is used as an intermediate variable for determining S_{Hmax} orientation. a is the geographic azimuth of the wellbore.
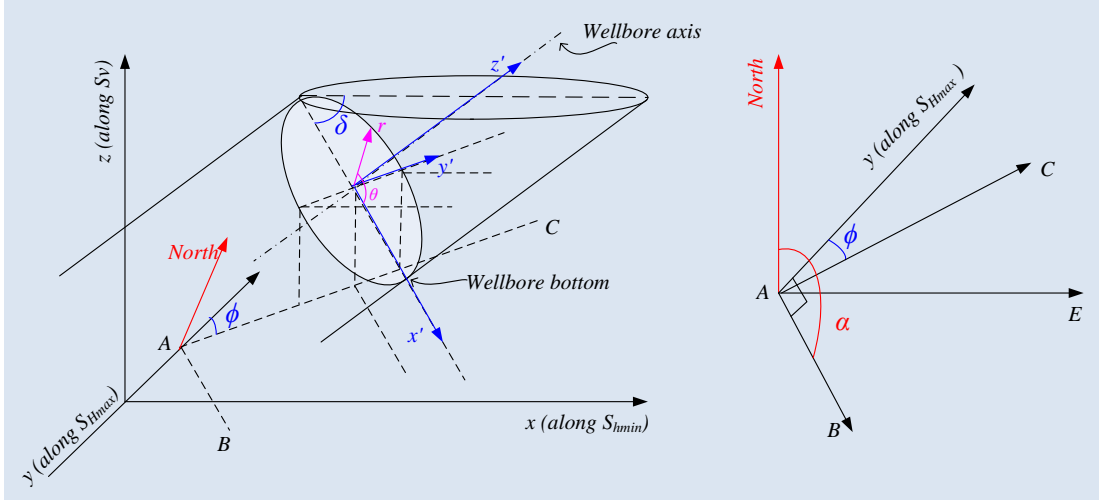
Figure 1 Different coordinate systems for this study

The in-situ principal stress tensor in *x-y-z* is given by:

$$
S_{ij} = \begin{bmatrix} S_h & & \\ & S_H & \\ & & S_v \end{bmatrix}
\tag{1}
$$

And the effective stress tensor is:

$$
S_{ij} = S_{ij} - bP_p d_{ij} = \begin{bmatrix} S_h & & \\ & S_H & \\ & & S_v \end{bmatrix} = \begin{bmatrix} S_h - bP_p & & \\ & S_H - bP_p & \\ & & S_v - bP_p \end{bmatrix}
\tag{2}
$$

where *b* is Biot coefficient, and P_p is the pore pressure.

The matrix for transforming the stress tensor from x-y-z into *x'-y'-z'* is thus:

$$
A = \begin{bmatrix} \cos d \cos f & -\cos d \sin f & -\sin d \\ \sin f & \cos f & 0 \\ \sin d \cos f & -\sin d \sin f & \cos d \end{bmatrix}
\tag{3}
$$

The effective stress tensor in x'-y'-z' is given by:

$$S_{i'j'} = AS_{ij}A^T = \begin{bmatrix} S_{x'x'} & S_{x'y'} & S_{x'z'} \\ S_{y'x'} & S_{y'y'} & S_{y'z'} \\ S_{z'x'} & S_{z'y'} & S_{z'z'} \end{bmatrix} \tag{4}$$

Here, the six independent stress components are:

$$S_{x'x'} = S_h \cos^2 d \cos^2 f + S_H \cos^2 d \sin^2 f + S_v \sin^2 d \tag{4.1}$$

$$S_{x'y'} = S_{y'x'} = (S_h - S_H)\cos d \sin f \cos f \tag{4.2}$$

$$S_{x'z'} = S_{z'x'} = S_h \sin d \cos d \cos^2 f + S_H \sin d \cos d \sin^2 f - S_v \sin d \cos d \tag{4.3}$$

$$S_{y'y'} = S_h \sin^2 f + S_H \cos^2 f \tag{4.4}$$

$$S_{y'z'} = S_{z'y'} = (S_h - S_H)\sin d \sin f \cos f \tag{4.5}$$

$$S_{z'z'} = S_h \sin^2 d \cos^2 f + S_H \sin^2 d \sin^2 f + S_v \cos^2 d \tag{4.6}$$

Normal stresses in r-θ-z' are:

$$S_{rr} = \frac{S_{x'x'} + S_{y'y'}}{2} + \frac{S_{x'x'} - S_{y'y'}}{2}\cos 2q + S_{x'y'}\sin 2q \tag{5.1}$$

$$S_{qq} = \frac{S_{x'x'} + S_{y'y'}}{2} - \frac{S_{x'x'} - S_{y'y'}}{2}\cos 2q - S_{x'y'}\sin 2q \tag{5.2}$$

$$S_{z'z'} = S_h \sin^2 d \cos^2 f + S_H \sin^2 d \sin^2 f + S_v \cos^2 d \tag{5.3}$$

After excavation of the wellbore, the re-distributed elastic stress state around the wellbore can be found using Kirsch solution (Kirsch, 1898). Here, we give the 3D solution by assuming plane strain along wellbore axis z':

$$S_{rr}^N = \frac{S_{x'x'} + S_{y'y'}}{2}\left[1 - \left(\frac{a}{r}\right)^2\right] + \frac{S_{x'x'} - S_{y'y'}}{2}\left[1 - 4\left(\frac{a}{r}\right)^2 + 3\left(\frac{a}{r}\right)^4\right]\cos 2q$$
$$+ S_{x'y'}\left[1 - 4\left(\frac{a}{r}\right)^2 + 3\left(\frac{a}{r}\right)^4\right]\sin 2q + P_{net}\left(\frac{a}{r}\right)^2 \tag{6.1}$$

$$S_{qq}^N = \frac{S_{x'x'} + S_{y'y'}}{2}\left[1 + \left(\frac{a}{r}\right)^2\right] - \frac{S_{x'x'} - S_{y'y'}}{2}\left[1 + 3\left(\frac{a}{r}\right)^4\right]\cos 2q$$
$$- S_{x'y'}\left[1 + 3\left(\frac{a}{r}\right)^4\right]\sin 2q - P_{net}\left(\frac{a}{r}\right)^2 \tag{6.2}$$

$$S_{z'z'}^N = S_{z'z'} - n\left[DS_{rr} + DS_{qq}\right] \tag{6.3}$$

$$S_{rq}^N = \frac{S_{y'y'} - S_{x'x'}}{2}\left[1 + 2\left(\frac{a}{r}\right)^2 - 3\left(\frac{a}{r}\right)^4\right]\sin 2q + S_{x'y'}\left[1 + 2\left(\frac{a}{r}\right)^2 - 3\left(\frac{a}{r}\right)^4\right]\cos 2q \tag{6.4}$$

$$S_{rz'}^N = \left(S_{x'z'}\cos q + S_{y'z'}\sin q\right)\left[1 - \left(\frac{a}{r}\right)^2\right] \tag{6.5}$$

$$S_{qz'}^N = \left(-S_{x'z'}\sin q + S_{y'z'}\cos q\right)\left[1 + \left(\frac{a}{r}\right)^2\right] \tag{6.6}$$

where ν is Poisson's ratio, P_{net} is difference between mud pressure P_{mud} and pore pressure P_p, and N indicates the new elastic stress state (redistributed) after excavation of wellbore. Note that E.q.(6.3) is a plane strain solution, where the change in radial normal stresses $\Delta\sigma_{rr}$ can be found by subtracting E.q.(5.1) from E.q.(6.1) , and the change in circumferential normal stress $\Delta\sigma_{\theta\theta}$ can be found by subtracting E.q.(5.2) from E.q.(6.2). This gives:

$$S_{z'z'}^{N} = S_{z'z'} - n\left[2\left(S_{x'x'} - S_{y'y'}\right)\left(\frac{a}{r}\right)^2 \cos 2q + 4S_{x'y'}\left(\frac{a}{r}\right)^2 \sin 2q\right] \tag{6.7}$$

On the wellbore wall, $a=r$, and the stress tensor simply reduces to:

$$S_{kl}^{N} = \begin{bmatrix} S_{rr}^{N} & 0 & 0 \\ 0 & S_{qq}^{N} & t_{qz'}^{N} \\ 0 & t_{qz'}^{N} & S_{z'z'}^{N} \end{bmatrix} \tag{7}$$

where

$$S_{rr}^{N} = P_{mud} - P_p = P_{net} \tag{7.1}$$

$$S_{qq}^{N} = S_{x'x'} + S_{y'y'} - 2\left(S_{x'x'} - S_{y'y'}\right)\cos 2q - 4S_{x'y'}\sin 2q - P_{net} \tag{7.2}$$

$$S_{z'z'}^{N} = S_{z'z'} - n\left[2\left(S_{x'x'} - S_{y'y'}\right)\cos 2q + 4S_{x'y'}\sin 2q\right] \tag{7.3}$$

$$t_{qz'}^{N} = 2\left[-S_{x'z'}\sin q + S_{y'z'}\cos q\right] \tag{7.4}$$

Substitute E.q.(4.1) ~ E.q.(4.6) into E.q.(7.2)~ E.q.(7.4), we obtain the elastic stress state on the wellbore expressed by a linear combination of the in-situ principal stresses and the net pressure:

$$\begin{bmatrix} S^N_{qq} \\ S^N_{z'z'} \\ t^N_{qz'} \end{bmatrix} = \begin{bmatrix} A_q & B_q & C_q & -1 \\ A_{z'} & B_{z'} & C_{z'} & 0 \\ A_{qz'} & B_{qz'} & C_{qz'} & 0 \end{bmatrix} \begin{bmatrix} S_h \\ S_H \\ S_v \\ P_{net} \end{bmatrix} \tag{8}$$

where

$$A_q = \left(1 - 2\cos 2q\right)\cos^2 d\cos^2 f + \left(1 + 2\cos 2q\right)\sin^2 f - 2\sin 2q\cos d\sin 2f \tag{8.1}$$

$$B_q = \left(1 - 2\cos 2q\right)\cos^2 d\sin^2 f + \left(1 + 2\cos 2q\right)\cos^2 f + 2\sin 2q\cos d\sin 2f \tag{8.2}$$

$$C_q = \left(1 - 2\cos 2q\right)\sin^2 d \tag{8.3}$$

$$A_{z'} = \sin^2 d\cos^2 f - 2n\cos 2q\cos^2 d\cos^2 f + 2n\cos 2q\sin^2 f - 2n\sin 2q\cos d\sin 2f \tag{8.4}$$

$$B_{z'} = \sin^2 d\sin^2 f - 2n\cos 2q\cos^2 d\sin^2 f + 2n\cos 2q\cos^2 f + 2n\sin 2q\cos d\sin 2f \tag{8.5}$$

$$C_{z'} = \cos^2 d - 2n\cos 2q\sin^2 d \tag{8.6}$$

$$A_{qz'} = -\sin q\sin 2d\cos^2 f + \cos q\sin d\sin 2f \tag{8.7}$$

$$B_{qz'} = -\sin q\sin 2d\sin^2 f - \cos q\sin d\sin 2f \tag{8.8}$$

$$C_{qz'} = \sin q\sin 2d \tag{8.9}$$

The three principal effective stresses on the wellbore wall are thus (not necessarily in the order of major, intermediate and minor):

$$S_1 = \frac{1}{2}\left(S_{qq}^N + S_{z'z'}^N\right) + \frac{1}{2}\sqrt{\left(S_{qq}^N + S_{z'z'}^N\right)^2 + 4\left(t_{qz'}^N\right)^2} \tag{9.1}$$

$$S_2 = \frac{1}{2}\left(S_{qq}^N + S_{z'z'}^N\right) - \frac{1}{2}\sqrt{\left(S_{qq}^N + S_{z'z'}^N\right)^2 + 4\left(t_{qz'}^N\right)^2} \tag{9.2}$$

$$S_3 = P_{net} \tag{9.3}$$

The first stress invariant and second deviatoric stress invariant are:

$$I_1 = S_{rr}^N + S_{qq}^N + S_{z'z'}^N \tag{10.1}$$

$$J_2 = \frac{1}{6}\left[\left(S_{rr}^N - S_{qq}^N\right)^2 + \left(S_{rr}^N - S_{z'z'}^N\right)^2 + \left(S_{qq}^N - S_{z'z'}^N\right)^2\right] + \left(t_{qz'}^N\right)^2 \tag{10.2}$$

3. SIMULTANEOUSLY DETERMINING THE MAGNITUDE AND ORIENTATION OF SHMAX AND ROCK STRENGTH USING BREAKOUTS IN DEVIATED WELLS

3.1 Assumptions

To carry out the new method, we make the following assumptions: (1) Wellbore breakout occurs at the region where stress state reaches certain failure criteria; (2) For simplification, the failure function is chosen to be a certain yield function, thus rock strength after yielding is neglected, and the size of the breakout coincides with the plastic yield zone; (3) Stress redistribution due to plastic strain is neglected; (4) Most importantly, the failure function reaches maximum value at breakout center, and reaches zero at breakout edges. Note that the last assumption does not conflict with the plastic consistency condition (Borja, 2013), which requires the yield function to remain zero since onset of yielding, as we are only concerned with the stress state during elastic prediction phase rather than plastic correction phase.

3.2 Developing a constrained optimization program

3.2.1 A constrained optimization problem

Under the above assumptions, our goal is to find the solution that maximized the failure function at the center of each picked breakout, while meeting other imposed conditions. Such is a constrained optimization problem, and can be described by:

$$\min obj(x) \tag{11.1}$$

Subjected to:

$$\begin{cases} c(x) \pounds 0 \\ ceq(x) = 0 \\ A \times x \pounds b \\ Aeq \times x = beq \\ lb \pounds x \pounds ub \end{cases} \tag{11.2}$$

where the five constraints are nonlinear inequality constraints, nonlinear equality constraints, linear inequality constrains, linear equality constraints, and lower and upper bound.

3.2.2 Yield criteria

For this study, we choose the circumscribed Drucker-Prager yield criterion that is suitable for compression representation (Drucker and Prager, 1952):

$$F(S_H, f, j, C, d, q) = \sqrt{J_2} - \left(aI_1 + k\right) \tag{12.1}$$

where

$$a = \frac{2\sin j}{\sqrt{3}(3 - \sin j)} \tag{12.2}$$

$$k = \frac{6C\cos\varphi}{\sqrt{3}(3-\sin\varphi)} \tag{12.3}$$

where C is the uniaxial compressive strength, and φ is the internal frictional angle.

3.2.3 Unknown vector

The unknown vector for this study is:

$$x = \begin{bmatrix} \partial_z\sigma_H \\ \phi \\ \varphi \\ C \end{bmatrix} \tag{13}$$

where: $\partial_z\sigma_H$ is the vertical gradient of effective maximum horizontal stress σ_H.

Note that the geographic azimuth of S$_{\text{Hmax}}$ can be calculated via:

$$azi = \alpha - \pi/2 - \phi \tag{14}$$

And the result will then be collapsed into [-90°, 90°], or [0, 180°], depending on the result, by adding or subtracting $n \cdot 180°$.

3.2.4 Objective function

In order to convert the problem into a minimization process, set the objective function as:

$$obj = -F(S_H, \phi, \varphi, C, d, q_p) = aI_1 - \sqrt{J_2} + k \tag{15}$$

where θ_p is the azimuth of the center of a picked breakout with respect to the wellbore bottom. This can be obtained during breakout picking by activating the wellbore-bottom coordinates.

3.2.5 Constraints

(1) Lower and upper bound

The lower and upper bounds of $\partial_z\sigma_H$ are imposed by the frictional strength of the earth crust (Townend and Zoback, 2000). Specifically, in our examples from the Vienna Basin (shown later), it is shown that the overburden S$_v$ derived from density logs is ubiquitously greater than S$_{hmin}$ measured by extended leak-off tests, suggesting the faulting regime is either normal or strike-slip. Thus the lower bound and upper bounds of $\partial_z\sigma_H$ are given by:

$$\partial_z\sigma_H \geq \partial_z\sigma_h \text{ (normal faulting regime)} \tag{16.1}$$

$$\partial_z\sigma_H \leq \left(\sqrt{\mu^2+1}+\mu\right)^2 \partial_z\sigma_h \text{ (strike-slip regime)} \tag{16.2}$$

where: $\partial_z\sigma_h$ is the gradient of effective S$_{hmin}$ over depth, and μ is the coefficient of friction.

The lower and upper bound of φ (angle between S$_{Hmax}$ and y') is 0 and 360°, as is shown in figure 1. Bounds of uniaxial compressive strength are estimated through log-derived UCS values. Here we select the following three empirical relations:

$$UCS = 143.8\exp(-6.95j) \tag{17.1}$$

$$UCS = 277\exp(-10j) \tag{17.2}$$

$$UCS = 135.9\exp(-4.8j) \tag{17.3}$$

Where φ is the porosity. In our case, the first two equations generally give a consistent lower bound, and the third equations gives an upper bound.

The internal frictional angle is generally between 35° and 42° (internal frictional angle between 0.7 and 0.9) for Vienna Basin, as are shown by some geomechanical reports.

(2) Nonlinear equality constrains:

The failure function at the wellbore breakout edges are used for setting up this constraint:

$$ceq(x) = \begin{bmatrix} F(\sigma_H, \phi, \varphi, C, \delta, \theta_{w1}) \\ F(\sigma_H, \phi, \varphi, C, \delta, \theta_{w2}) \end{bmatrix} \tag{18.1}$$

where

$$\theta_{w1} = \theta_p - width/2 \tag{18.2}$$

$$\theta_{w2} = \theta_p + width/2 \tag{18.3}$$

where, *width* refers to the angular width of a picked breakout.

(3) Nonlinear inequality constraints:

Nonlinear inequality constraint is given based on the presence or lack of drilling induced tensile fracture at each breakout depth. We calculate stress state ±90° away from picked breakout center, and employ the 3D Griffith tensile failure criterion (Griffith, 1921) :

If there are drilling induced tensile fractures:

$$FT(S_H, f, j, C, d, q_{w3,w4}) = \begin{cases} -\left(\dfrac{(S_1 - S_3)^2}{S_1 + S_3} - 8S_t \right) < 0, & if\ S_1 + 3S_3 \geq 0 \\ S_3 + S_t < 0, & if\ S_1 + 3S_3 < 0 \end{cases} \tag{19.1}$$

If there are no drilling induced tensile fractures:

$$FT(S_H, f, j, C, d, q_{w3,w4}) = \begin{cases} \dfrac{(S_1 - S_3)^2}{S_1 + S_3} - 8S_t < 0, & if\ S_1 + 3S_3 \geq 0 \\ -\left(S_3 + S_t \right) < 0, & if\ S_1 + 3S_3 < 0 \end{cases} \tag{19.2}$$

where:

$$\theta_{w3} = \theta_p - \pi/2 \tag{19.3}$$

$$\theta_{w4} = \theta_p + \pi/2 \qquad , \tag{19.4}$$

And the three effective principal stresses σ_1, σ_2, σ_3 are in the order of major, intermediate and minor. The nonlinear inequality function is then:

$$c(x) = \begin{bmatrix} FT(\sigma_H, \phi, \varphi, C, \delta, \theta_{w3}) \\ FT(\sigma_H, \phi, \varphi, C, \delta, \theta_{w4}) \end{bmatrix} \tag{20}$$

(4) Linear equality and inequality constraints

Linear constraints are set to null in this study.

3.2.6 Optimization process

We use an 'interior point' algorithm for performing the optimization, and during each iteration, we compute the Hessain Matrix (for second derivative test) using the Quasi-Newton method, and at each breakout depth, we select only the result that satisfies (to ensure the optimized result is a local mimimum):

$$det\left(Hessian\right) > 0 \tag{21}$$

The following flowchart summarizes the optimization process.
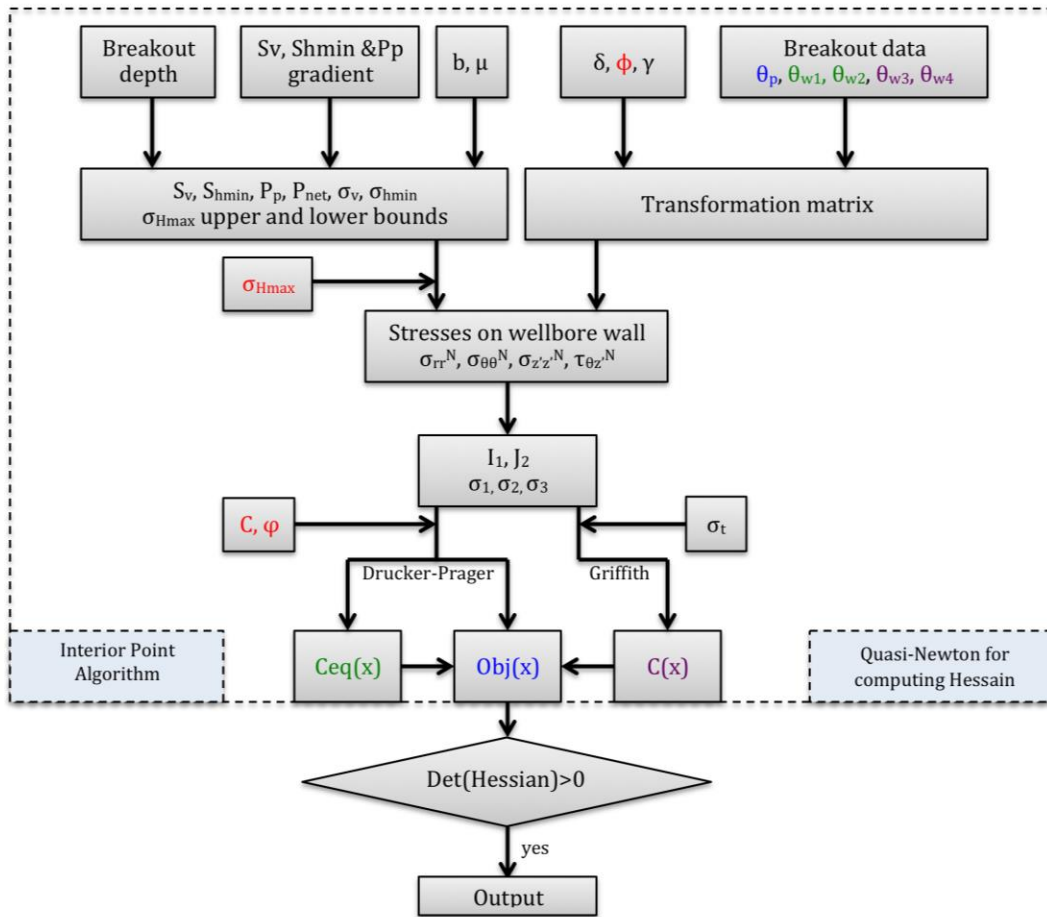
Figure 2: Flow chart showing the set-up of the optimization problem. The primary unknowns, including the magnitude of effective SHmax, the orientation-related angle, the uniaxial compressive strength and the internal frictional angle, are marked with red. Independent knowledge of S_v, S_{hmin} and P_p are required for deriving the upper and lower limit of S_{Hmax} by imposing frictional equilibrium. Wellbore trajectory with respect to stress field, in conjunction with location on the wellbore, is used for transforming the in-situ stress tensor into stresses around the wellbore. The Drucker-Prager yield criterion is used for formulating the objective function (blue) and the nonlinear equality constraints (green), and the 3D Griffith tensile failure criterion is used for formulating the nonlinear inequality constraints (purple). A second-derivative test is enforced at the end for selection of local extremum (minimum). The process is easily repeatable for all breakouts.

4. METHOD SIMPLICAFTION FOR VERTICAL WELLS

The method for determining the magnitude of S_{Hmax} and the rock strength using breakouts in vertical wells is similar to that for deviated wells, except that the orientation of S_{Hmax} is known

(S_{Hmax} azimuth always ±90° from breakout center azimuth in vertical wells), so the unknown vector x becomes:

$$x = \begin{bmatrix} \partial_z \sigma_H \\ \varphi \\ C \end{bmatrix} \tag{22}$$

Stresses on a vertical cylindrical wellbore are (all shear stresses vanish):

$$S_{rr}^N = P_{net} \tag{23.1}$$

$$S_{qq}^N = S_h + S_H - 2(S_h - S_H)\cos 2q - P_{net} \tag{23.2}$$

$$S_{z'z'}^N = S_v - 2n(S_h - S_H)\cos 2q \tag{23.3}$$

where θ is the angle with respect to the S_{hmin} direction in anti-clockwise sense.

Having the wellbore stresses, we can construct the objective function and impose the constraints in a similar manner to that described above before performing the optimization.

5. EXAMPLE

We select a deviated well located in east Vienna Basin for demonstration of the new method.

Table 1: A list of the input parameters for optimization

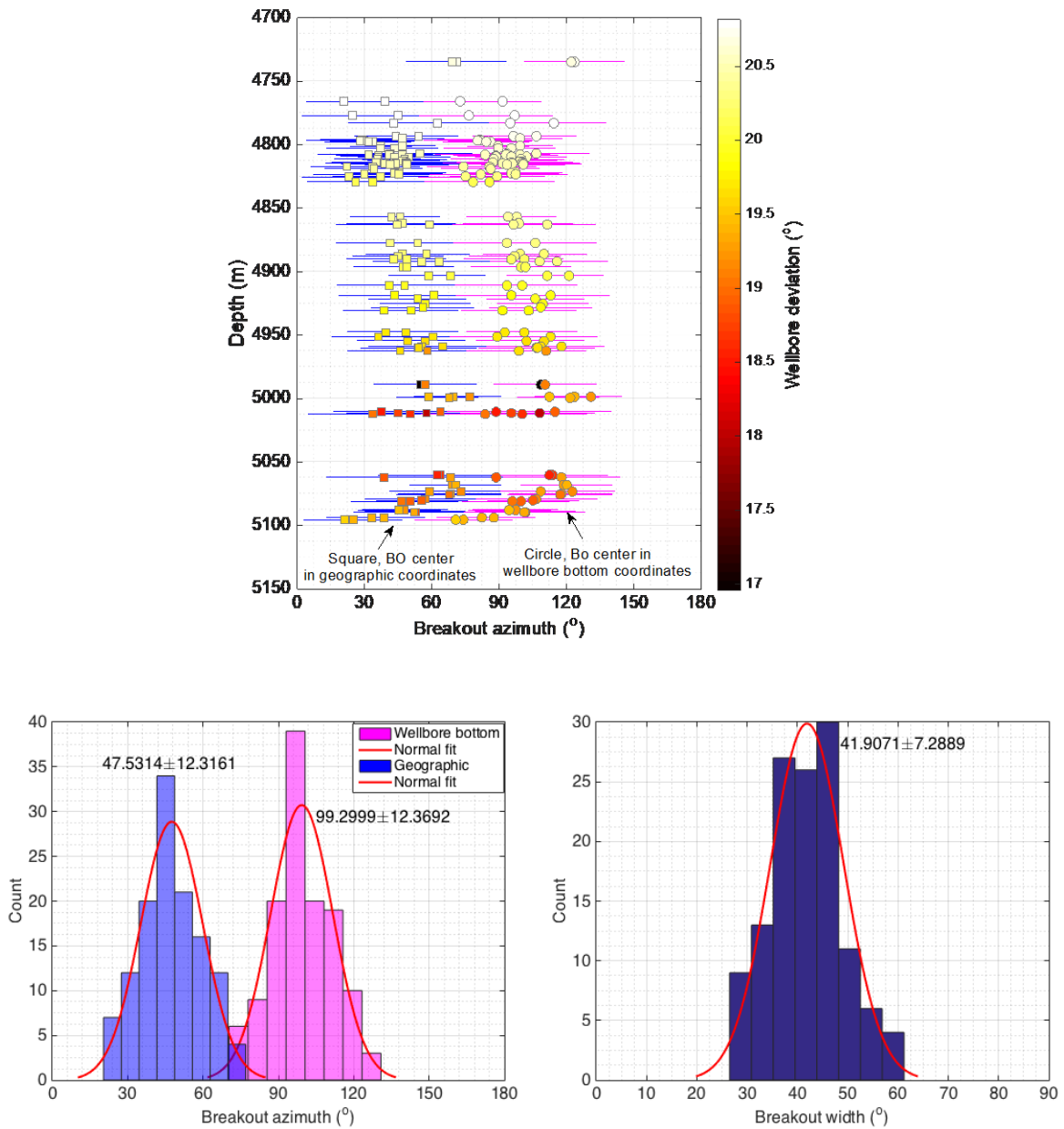| Input parameter	Value	Comments
S_v	0.251 bar/m	Integration over density log
S_{hmin}	0.188 bar/m	Extended leak-off test
P_p	0.098 bar/m	Hydrostatic
P_{net}	$0.1P_p$	From drilling report
μ	0.6	--
b	1	--
γ	0.25	--
σ_t	$C/8$	Predicted by the 3D Griffith tensile failure criterion

Figure 3: Picked breakout data from the selected deviated well as inputs for optimization. Upper: breakout profile with depth, plotted in both wellbore bottom coordinates (for optimization) and in geographic coodinates (for post-processing), colored by wellbore deviation. Bars indicate breakout widths; Lowerleft: histogram and normal fit of breakout azimuth with respect to wellbore bottom and geographic north; Lowerright: histogram and normal fit of breakout width.
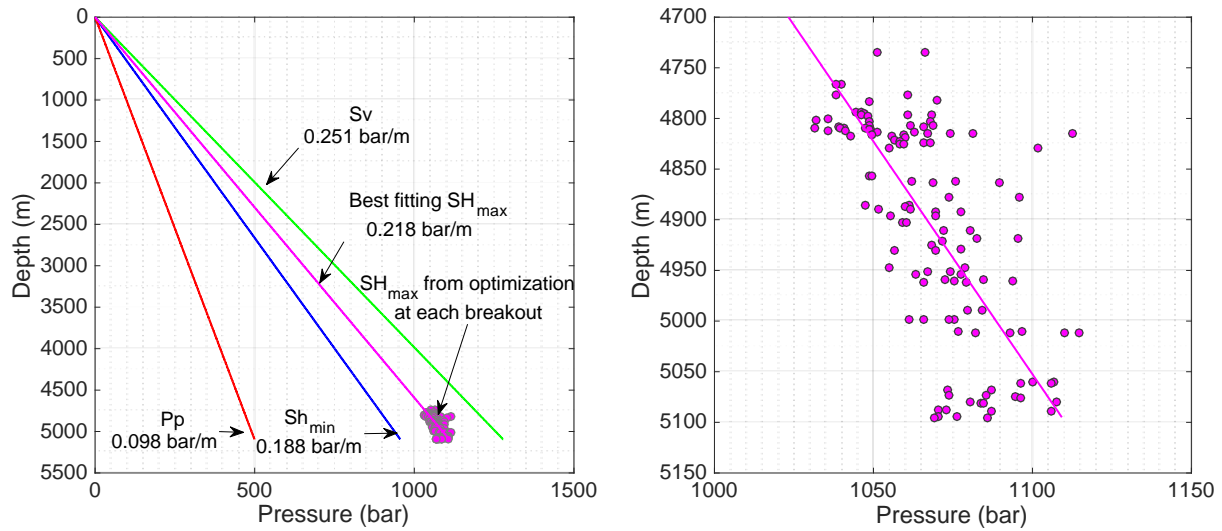
Figure 4: Geomechanical model for the example. Overburden (green) is derived from density log, Shmin (blue) is measured from extended-leak-off test, and pore pressure (red) is hydrostatic. The optimized S_{Hmax} magnitudes from all breakouts are shown, and a best-fitting line is also given. Left: Global view; Right: a close-up view.
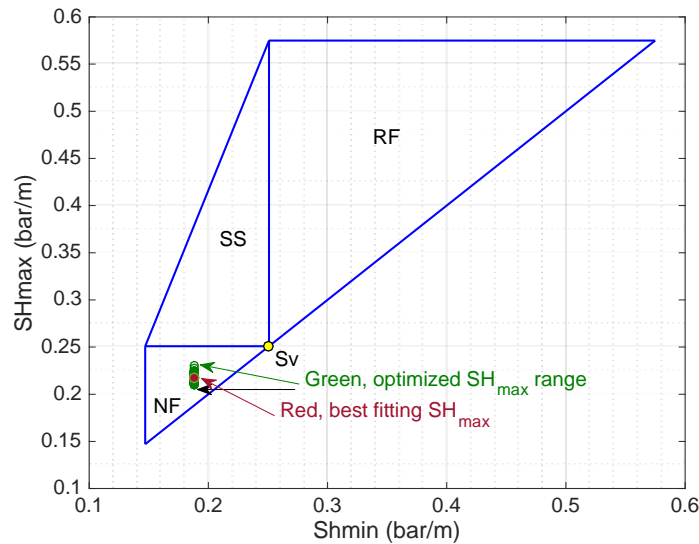

Figure 5: Optimized SHmax magnitudes from all picked wellbore breakout (green), plotted on a stress polygon. Red dot indicates the best fitting data. The result definitively suggests a normal faulting regime.
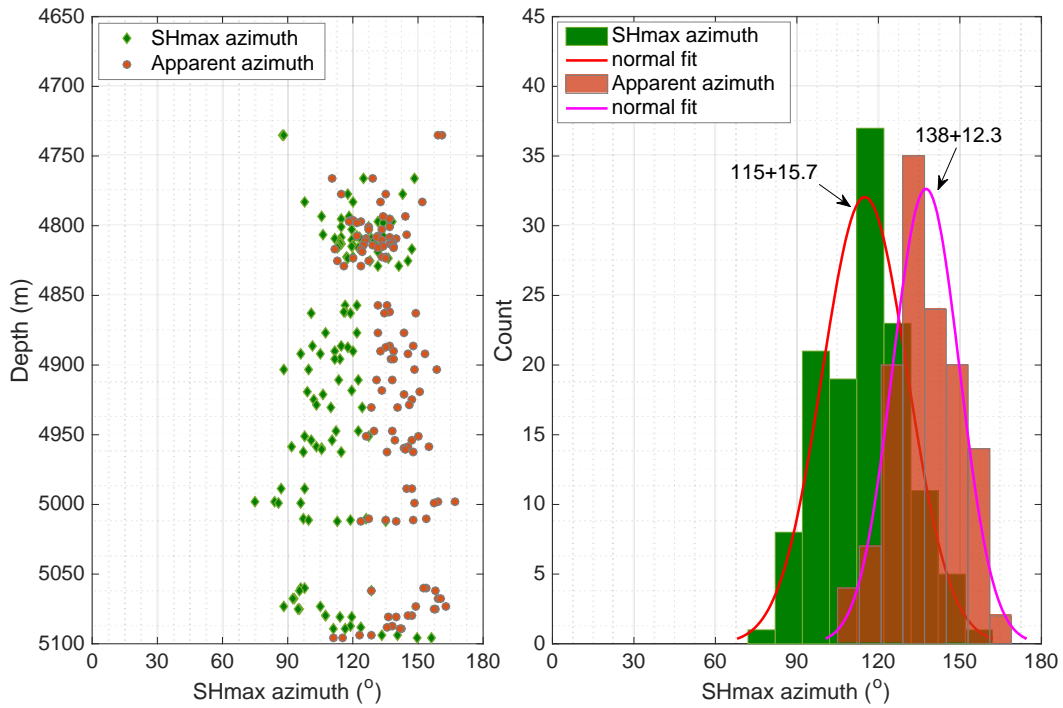
Figure 6: Left: Optimized SHmax azimuth profile with depth, contrasted with the apparent SHmax azimuth profile (without considering the impact of welllbore trajectory) with depth; Right: histogram and normal fit of optimized SHmax azimuth, compared to those of the apparent SHmax azimuth, showing an over 20° difference in the mean value.
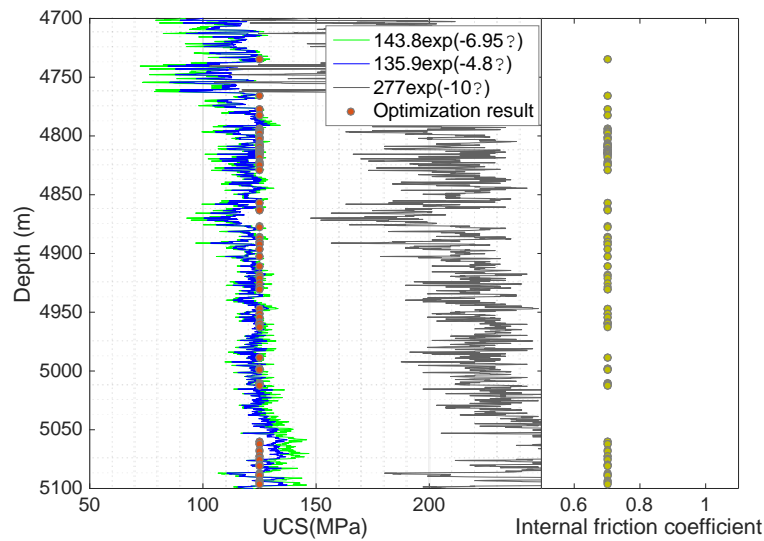
Figure 7: Optimized rock strength; Left: UCS, compared with the profiles derived from the porosity log using selected empirical relations; Right: internal frictional angle. Optimization result suggests depth-invariant UCS and internal frictional angle profile within the interval of study.

6. CONCLUSION

We developed a new method for simultaneously determine the magnitude and orientation of S_{Hmax}, as well as two rock strength parameters, including UCS and internal frictional angle, using drilling-induced wellbore failures in arbitrarily oriented wells. The new method transforms the conventional forward approach into a constrained optimization process by utilizing the information previously not considered: the redistributed elastic stress state maximizes the failure function at the center of a breakout. Our method overcomes several limitations imposed on the conventional approach. It does not required the orientation of S_{Hmax} and rock strength to be known *a priori*, and fully accounts for the inter-dependence among the primary unknowns, and fully considers the impact of wellbore trajectory on wellbore failures. This method is especially useful when breakout data is available only in deviated wells and S_{Hmax} orientation cannot be independently determined. In addition, compared to the conventional approach, the new method is easily repeatable for all breakouts, and is more practical when dealing with large quantities of breakout data.

ACKNOWLEDGEMENTS

REFERENCES

1. Barton, C. A., Castillo, D. A., Moos, D., Peska, P., & Zoback, M. D. (1998). Characterising the full stress tensor based on observations of drilling-induced wellbore failures in vertical and inclined boreholes leading to improved wellbore stability and permeability prediction. APPEA J, 38(1), 466-487.

2. Della Vecchia, G., Pandolfi, A., Musso, G., & Capasso, G. (2014). An analytical expression for the determination of in situ stress state from borehole data accounting for breakout size. International journal of rock mechanics and mining sciences, 66, 64-68.

3. Townend, J., & Zoback, M. D. (2000). How faulting keeps the crust strong.Geology, 28(5), 399-402.

4. Zoback, M. D. (2010). Reservoir geomechanics. Cambridge University Press.

5. Peška, P., & Zoback, M. D. (1995). Compressive and tensile failure of inclined well bores and determination of in situ stress and rock strength. Journal of Geophysical Research: Solid Earth (1978–2012), 100(B7), 12791-12811.

6. Mastin, L. (1988). Effect of borehole deviation on breakout orientations. Journal of Geophysical Research: Solid Earth (1978–2012), 93(B8), 9187-9195.

7. Zajac, B. J., & Stock, J. M. (1997). Using borehole breakouts to constrain the complete stress tensor: Results from the Sijan Deep Drilling Project and offshore Santa Maria Basin, California. Journal of Geophysical Research: Solid Earth (1978–2012), 102(B5), 10083-10100.

8. Djurhuus, J., & Aadnøy, B. S. (2003). In situ stress state from inversion of fracturing data from oil wells and borehole image logs. Journal of Petroleum Science and Engineering, 38(3), 121-130.

9. Thorsen, K. (2011). In situ stress estimation using borehole failures - Even for inclined stress tensor. Journal of Petroleum Science and Engineering, 79(3), 86-100.

10. Kirsch (1898). Die Theorie der Elastizität und die Bedürfnisse der Festigkeitslehre. Zeitschrift des Vereines deutscher Ingenieure, 42, 797–807.

11. Borja, R. I. (2013). Plasticity. Springer.

12. Drucker, D. C. and Prager, W. (1952). Soil mechanics and plastic analysis for limit design. Quarterly of Applied Mathematics, vol. 10, no. 2, pp. 157–165.

13. Griffith, A. A. (1921). The phenomena of rupture and flow in solids.Philosophical transactions of the royal society of london. Series A, containing papers of a mathematical or physical character, 163-198.